

Ciprofloxacin loaded calcium alginate wafers prepared by freeze-drying technique for potential healing of chronic diabetic foot ulcers

Asif Ahmed, Giulia Getti, Joshua Boateng*

Department of Pharmaceutical, Chemical & Environmental Sciences, Faculty of Engineering and Science, University of Greenwich, Medway, Central Ave. Chatham Maritime, Kent ME4 4TB, UK.

* Correspondence: Dr Joshua Boateng (j.s.boateng@gre.ac.uk; joshboat40@gmail.com)

Abstract

Calcium alginate (CA) wafer dressings were prepared by lyophilization of hydrogels to deliver ciprofloxacin (CIP) directly to the wound site of infected diabetic foot ulcers (DFUs). The dressings were physically characterized by scanning electron microscopy (SEM), texture analysis (for mechanical and *in-vitro* adhesion properties), X-ray diffraction (XRD), Fourier transform infrared spectroscopy (FTIR). Further, functional properties essential for wound healing i.e. porosity, *in-vitro* swelling index, water absorption (A_w), equilibrium water content (EWC), water vapor transmission rate (WVTR), evaporative water loss (EWL), moisture content, *in vitro* drug release and kinetics, antimicrobial activity and cell viability (MTT assay) were investigated. The wafers were soft, of uniform texture and thickness and pliable in nature. Wafers showed ideal wound dressing characteristics in terms of fluid handling properties due to high porosity (SEM). XRD confirmed crystalline nature of the dressings and FTIR showed hydrogen bond formation between CA and CIP. The dressings showed initial fast release followed by sustained drug release which can inhibit and prevent re-infection caused by both Gram-positive and Gram-negative bacteria. The dressings also showed biocompatibility (> 85% cell viability over 72 h) with human adult keratinocytes. Therefore, it will be a potential medicated dressing for patients with DFUs infected with drug resistant bacteria.

Keywords: Calcium alginate; Ciprofloxacin; Diabetic foot ulcer; Infection; Lyophilized wafer; Wound healing

1. Introduction

Chronic wounds arise from tissue injuries or disruption to anatomical structures that heal beyond 12 weeks [1]. They are associated with predisposing factors that might disturb the balance between wound bioburden and the patient's immune system or hinder the wound healing cycle [2]. The incidence of chronic wounds including diabetic foot, leg, pressure, venous and arterial ulcers as well as trauma, has increased significantly in recent years due to obesity, aging, high alcohol consumption, smoking, stress, poor nutrition, diabetic mellitus, ischemia, venous stasis disease, and high blood pressure [3].

Diabetic foot ulcers (DFUs) are one of the most common causes of morbidity and high risk of lower extremity amputation in diabetic patients [4]. Worldwide, an estimated 15% of diabetic patients are affected by DFUs in their lifetime and this has a high cost burden for national health providers [5]. For example in England alone, DFUs and associated amputations cost taxpayers approximately £972 million to £1.13 billion in 2014-15 which is equivalent to 0.72-0.83% of the entire budget of the National Health Service [6]. Diabetic patients are susceptible to infections of foot ulcers due to peripheral neuropathy and peripheral vascular disease resulting in poor circulation and weakened neutrophil function [7]. The foot ulcerations are therefore prone to colonization by various pathogenic organisms including *Staphylococcus aureus*, *Streptococcus group B*, *Enterococcus*, *Clostridium perfringens*, *Enterobacteriaceae*, *Pseudomonas* and *Stenotrophomonas maltophilia*. *Staphylococcus aureus* is the most common bacteria in DFUs and about 50% of isolates were methicillin-resistant *S. aureus* (MRSA) [8,9]. High microbial load and the presence of drug resistant bacteria retard the healing process of DFUs, which increases the rate of amputation and mortality [10].

There are many therapies for DFUs with wound dressings being one of them [11]. Current dressings such as hydrogels, hydrocolloids and films available for treating DFUs are generally ineffective and no single dressing can fulfil all the requirements for effective treatment of DFUs [12]. These dressings struggle to effectively heal highly exuding wounds such as DFUs and venous leg ulcers (VLUs) because of inability to absorb and high amount of exudates. On the other hand foam, gauze, bandage, sponge and fiber mats are associated with pain and patient discomfort during removal. These dressings can also cause dermatitis due to adherence to the wound which leads to wound debridement and thereby delaying wound healing process [12-15]. Moreover, bioactive dressings such as collagen, hyaluronic acid and elastin are expensive. In addition, most of the antibiotic agents used in DFUs are administered via the IV route which is inconvenient and leads to non-compliance [16-20]. Furthermore, due

to poor circulation at the extremities of diabetic patients, systemic antibiotic treatment is largely ineffective and direct delivery to the wound site is required. Antibiotics are sometimes incorporated into semi solid formulations (creams, gels and ointments) that are applied directly to the wounds to prevent or control infections. However, these dressings have major limitations due to their inability to maintain effective drug concentration for a prolonged period at the moist wound surface because of short residence time. These semi solid formulations absorb fluid rapidly and therefore, become mobile due to loss of rheological properties [12].

Lyophilized wafers have been reported as one of the most advanced dressings as drug delivery systems to wounds [21–23]. Due to their highly porous nature, wafers can absorb large amounts of heavy exudate whilst maintaining a moist environment without damaging newly formed tissue that improves wound healing [23]. Generally, chronic ulcers such as DFUs produce significant amounts of such exudate which can form slough and such collection of exudate under a dressing can cause maceration of surrounding healthy skin and also be a conducive environment for infection. The porosity of the wafers also allows gaseous (water vapor) exchange which enables evaporation of wound exudates through the polymeric matrix to the surrounding environment, thus preventing fluid accumulation under the dressing and subsequently reducing the risk of skin maceration and also controlling infections. It has been reported that wafers have excellent physicochemical properties in terms of swelling, diffusion, wound adhesion, drug stability and drug loading capacity [21,23–26]. Furthermore, wafers can be loaded with multiple drugs simultaneously, which imparts multifunctional effects [23] and are a compatible delivery system to carry both insoluble and soluble antimicrobial drugs which imparts better antimicrobial activity [22]. Wafers can be easily applied to the wounds because of its soft, uniform texture and pliable nature. When wafers are applied to the wound site, they absorb wound fluids and are transformed into a gel which provides moist environment and facilitating pain free removal of the dressings unlike foam or gauze, thereby increasing patient compliance [27]. Moreover, the controlled or sustained release of antibiotics from wafers may overcome the problem of uncontrolled release of drugs from the traditional dressings such as creams and ointments [26, 28]. In addition, medicated lyophilized wafers can reduce the cost burden for routine chronic wound healing, because of relatively low manufacturing costs [29] compared to other modern dressings such as tissue engineered skin substitutes.

Ciprofloxacin (CIP), a second-generation fluoroquinolone derivative, has been shown to be highly effective against both Gram positive and Gram negative bacteria both of which are

commonly found in infected wounds. Because of its low minimum inhibitory concentration (MIC), it has become a promising drug to incorporate into polymeric dressings for the potential treatment of chronic wounds [30-37]. Antibiotics loaded dressings have great advantages of avoiding systemic side effects; interference with wound healing and drug resistance [38]. Serious adverse effects of systemically administered CIP has been reported [39] which creates the need to develop CIP dressings for local application as an alternative way for healing of DFUs.

Calcium alginate (CA), a calcium salt of alginic acid, is extracted from brown seaweed and is made up of alternating sequences of β -(1-4) D-mannuronic acid (M-blocks) and α -(1-4) L-guluronic acid (G-blocks). The proportional distribution of the blocks depends on the origin and the part of the seaweed used with the mannuronic and guluronic acid residues adopting different conformational structures [40]. It has been found by conformational analysis that the di-equatorial mannuronic acid residues in M-block exhibit flexible flat ribbon-like chain conformation whilst the di-axially linked guluronic acid residues in G-block show rigid structures [41]. Calcium alginate has been widely used in highly exuding wounds such as DFUs and pressure and leg ulcers due to its hemostatic properties. It exchanges calcium ions with sodium ions present in the blood (wound exudate) and this stimulates growth factors including platelet-derived growth factors and cytokines which play a vital role in cell recruitment and extracellular matrix deposition [42]. It has been reported as biocompatible, bioadhesive, has high water absorption capacity, potential carrier for control drug release and non-toxic to cells [43,44]. *In vitro* wound healing capacity testing of calcium alginate based nano fiber bandage in rat model confirmed it as an excellent dressing material [45]. Various commercially available silver incorporated calcium alginate based dressings have been indicated for DFUs including Algisite Ag[®], Sorbalgon Ag[®], Gentell Calcium Alginate Ag[®], and Suprasorb A + Ag Calcium Alginate[®] [2,46]. However, silver-impregnated dressings have been reported to be cytotoxic to keratinocytes and fibroblasts, and delay wound healing in animal wound models [47–49]. A Cochrane review of silver based dressings concluded that silver dressings do not improve healing of DFUs [50]. Therefore, antibiotic loaded dressings can be an alternative way of healing DFUs.

This study therefore aims to formulate and characterize medicated advanced dressings in the form of lyophilized wafers to deliver therapeutically relevant doses of a broad-spectrum antibiotic (CIP) directly to the wound site of infected DFUs. The formulated wafers were physically characterized by scanning electron microscopy (SEM), X-ray diffraction (XRD), Fourier transform infrared spectroscopy (FTIR) and texture analysis (for mechanical

hardness and *in-vitro* adhesion). The dressings were further functionally characterized for fluid handling properties by *in-vitro* swelling studies, moisture content, equilibrium water content (EWC), water absorption (Aw), water vapor transmission rate (WVTR), porosity and evaporative water loss. *In vitro* antimicrobial and cell viability studies were performed to test the antimicrobial activity and biocompatibility of the wafers respectively. Further, the fluid (exudate) handling and biological properties including antimicrobial and cell viability studies of the dressings were compared with a commercial silver incorporated CA based antimicrobial dressing, Algisite Ag[®].

2. Materials and methods

2.1. Materials

Calcium alginate (mannuronic acid: guluronic acid ratio 59:41) [CA, (lot number: BCBM8132V)], Ciprofloxacin [CIP, (lot number: LRAA6508)], Mueller hinton broth [MH, (lot number: BCBR1543V)], tris(hydroxymethyl)aminomethane (lot number: SLBH9329V), Dulbecco's phosphate buffered saline [D-PBS, (lot number: RNBD8494)], trypsin-EDTA solution (lot number: SLBM8412V) and fetal bovine serum [FBS, (lot number: 045M3318)] were purchased from Sigma-Aldrich (Gillingham, UK). Agar [agar no. 3, technical, (lot number: 1334018)], sodium carbonate (lot number: 1546575), sodium chloride (lot number: 1560652), bovine serum albumin [BSA, (lot number: 1158022)], hydrochloric acid [HCl, (lot number: 1480980)], ethanol (batch number: 0933421) and dimethyl sulfoxide [DMSO, (batch number: 0890132)] were ordered from Fisher Scientific (Loughborough, UK). *Escherichia coli* (ATCC 25922), *Staphylococcus aureus* (ATCC 29213) and *Pseudomonas aeruginosa* (ATCC 27853) were obtained from the microbiology lab of the University of Greenwich, UK. Adult human primary epidermal keratinocytes (PCS-200-011, ATCC), dermal cell basal medium (PCS-200-030, ATCC) and keratinocytes growth kit (PCS-200-040, ATCC) were purchased from LGC standards (Middlesex, UK). Methylthiazolyldiphenyl-tetrazolium bromide [MTT, (lot number: 1721505)] and trypan blue stain, 0.4% (lot number: 1696154) were obtained from Thermo Fisher Scientific (Paisley, UK).

2.2. Preparation of polymer gels

The blank (BLK) polymeric gels comprising of CA (0.5 - 2% w/w) were prepared by adding the polymer powder in tiny amounts into the vortex of a vigorously stirred 0.014 M sodium carbonate solution at 50°C to avoid lump formation. In the case of drug loaded (DL) gels, stock solution of CIP was initially prepared at a concentration of 20 mg/ml in 0.1 N hydrochloric (HCl). The stock solution was further diluted with 0.014 M sodium carbonate to achieve working stock solution at a concentration of 1 mg/ml. Different volumes of the working stock of CIP were added to the BLK gels (1% w/w) to achieve drug concentration of 0.0001-0.0400% w/v in the gel.

2.3. Preparation of lyophilized wafers

To obtain wafers, 1 g each of the above formulated gels were poured into 24 well plate (diameter 15.6 mm) (Corning® Costar® cell culture plates; Sigma-Aldrich) and freeze-dried using a Virtis Advantage XL 70 freeze dryer (Biopharma Process System, Winchester, UK) in automatic mode. A previously reported lyophilisation cycle was adapted to prepare wafers [23]. In brief, the samples were cooled to -5°C from room temperature for 1 h, and further frozen at -50°C for 8 h (at 200 mTorr). The frozen samples were then primary dried to -25°C (at 50 mTorr) in a sequence of thermal ramps for 24 h, followed by secondary drying at 20°C (at 10 mTorr) for 7 h.

2.4. Scanning electron microscopy (SEM)

SEM was used to analyze the surface morphology of the wafers using a Hitachi SU 8030 (Hitachi High-Technologies, Germany) scanning electron microscope at low accelerating voltage (1.0 kV). The wafers were cut into small pieces, and attached to aluminium stubs (15 mm diameter), with the help of double-sided adhesive carbon tape (Agar Scientific G3357N). After that, wafers were carbon coated before visualization in the microscope. The images of BLK and DL wafers were captured at working distances of 18.4 mm and 8.3 mm respectively at a magnification of x200 using i-scan 2000 software.

2.5 Texture analysis

2.5.1. Mechanical hardness

The hardness (resistance to compressive deformation and ease of recovery) of the wafers was investigated by using a TA HD Texture analyzer (Stable Microsystem Ltd., Surrey, UK) fitted with a 5 kg load cell and *Texture Exponent 32* software program to plot

and display data. The average thickness (5-6 mm) of the wafers measured by a digital Vernier caliper electronic micrometer gauge (one in the middle and four edges) was entered into the software before compression. The instrument was set to compression mode and height of the 6 mm diameter (p/6) cylindrical stainless steel probe calibrated prior to compression. Three different wafers of each formulation ($n = 3$) were compressed by the probe at three different places, on both sides of the wafers using a trigger force of 0.001 N, to a depth of 2 mm, at a speed of 1 mm/sec, with a 10 mm return distance [21]. The BLK and DL wafers were evaluated to determine the effect of increasing drug content on flexibility to select optimum drug loading.

2.5.2. *In-vitro* adhesion studies

In-vitro adhesion of the wafers was investigated using the same texture analyzer and software program mentioned above (section 2.5.1). In this test, a 35 mm diameter (p/35) cylindrical stainless steel probe was attached to the wafers using double-sided adhesive tape. To represent chronic wound surface, 500 μ l of simulated wound fluid (SWF) containing either 2% (w/w) BSA or 5% (w/w) BSA was spread over set gelatin (6.67% w/w) gel. The wafer fitted with the probe was lowered until it made contact with the surface of the gelatin gel. The texture analyzer was set to run in tensile mode; followed by 60 s contact time with an applied force of 1 N and detached at a pre-test and test speed of 0.5 mm/s and post-test speed of 1 mm/s, 0.05 N trigger force and 10 mm return distance. The maximum force required to separate wafers from the surface of gelatin gel, the area under the curve of force versus distance and the total distance (in mm) travelled by wafers till complete separation were recorded to represent stickiness (peak adhesive force), total work of adhesion (WOA) and cohesiveness respectively. Each formulation was tested in triplicate ($n = 3$).

2.6. *X-ray* diffraction (XRD)

XRD was used to investigate the physical form (amorphous or crystalline) of the pure drug, polymer, BLK and DL wafers. The wafers were compressed with a glass slide to cover the round tiles of the holder and tightly attached to the sample cells with the help of transparent plastic cling film. The experiment was performed using a D8 Advance X-ray diffractometer (Bruker, Germany) in transmission mode. The instrument was set at a voltage and current of 40 kV and 40 mA, respectively with a primary solar slit of 4° and a secondary solar slit of 2.5° whereas the exit slit was 0.6 mm. Lynx Eye silicon strip position sensitive

detector was set with an opening of 3° and the Lynx Iris was set at 6.5 mm. The samples were scanned between 2 theta scale of 10-50° at a rotation speed of 15 rpm. The step size was 0.02° and counting time was 0.1 s per step.

2.7 Fluid (exudate) handling properties

2.7.1 Porosity

The porosity of wafers and commercial product, fiber mat (Algisite Ag®) was determined by the solvent displacement method as previously described [51]. The geometrical dimensions (thickness and diameter) of samples were measured by a digital Vernier caliper electronic micrometer gauge and total pore volume (V_0) was calculated. After that, samples were weighed (W_0) before immersing in 10 ml of ethanol for 3 h to reach saturation. Ethanol displaced the void space of wafers. Finally, the samples were carefully removed from the solvent, blotted with tissue paper to remove excess solvent and immediately weighed (W_1) to avoid loss of ethanol because of its volatile nature. The porosity of the dressings was calculated from equation 1.

$$\text{Porosity (\%)} = (W_1 - W_0) / (\rho_{eth} V_0) \times 100 \quad (1)$$

ρ_{eth} : density of ethanol = 0.789 g/cm³

2.7.2 Water absorption, equilibrium water content and swelling index

Water absorption (A_w) and equilibrium water content (EWC) tests were performed to investigate the maximum water uptake and water holding capacities respectively of the dressings. In addition, swelling studies were undertaken to investigate the rate of water uptake capacity of formulated BLK and CIP loaded wafers compared with a commercial fiber mat, Algisite Ag® (Smith & Nephew, UK). The A_w , EWC and swelling tests of all samples were investigated in simulated wound fluid (SWF) containing 2% (w/w) bovine serum albumin (BSA), 0.02 M calcium chloride, 0.4 M sodium chloride, 0.08 M tris (hydroxymethyl) aminomethane in deionized water at a pH of 7.5. For A_w and EWC studies, the samples were incubated in 10 ml of SWF at 37°C continuously for 24 h. In the case of swelling test, the samples were dipped into the same amount of SWF at room temperature and the changes in weight of swollen samples were recorded every 15 min up to 1 h and then every hour up to 5 h. Before weighing, the samples were blotted carefully with tissue paper to remove excess fluid on the surface. The effect of drug concentration on the above properties was determined and the experiments were performed in triplicate ($n = 3$) for each

sample. Percentage of Aw, EWC and swelling index (Is) were calculated using equations 2, 3 and 4 respectively.

$$Aw(\%) = \frac{W_s - W_i}{W_i} \times 100 \quad (2)$$

$$EWC(\%) = \frac{W_s - W_i}{W_s} \times 100 \quad (3)$$

Where W_s and W_i are the swollen weight and the initial weight before immersed into SWF respectively.

$$Is(\%) = \frac{W_{st} - W_d}{W_d} \times 100 \quad (4)$$

Where W_d is the dry weight of samples before hydration and W_{st} is the swollen weight of samples at different time of hydration.

2.7.3 Water vapor transmission rate

Using 90-second epoxy glue, the dressings were mounted on the mouth of a cylindrical plastic tube (15 mm diameter) containing 4 ml water with 8 mm air gap between the samples and water surface. The whole setup was placed in an air-circulated oven at 37°C for 24 h. The WVTR was calculated using equation 5:

$$WVTR = \frac{W_i - W_t}{A} \times 10^6 \text{ g/m}^2 \text{ day}^{-1} \quad (5)$$

Where A is the area of the mouth of the plastic tube (πr^2), W_i and W_t are the weight of the whole setup before and after placing into oven respectively.

2.7.4 Evaporative water loss

The samples were immersed in SWF and kept in an oven at 37°C for 24 h after which the samples were taken out, and dried in the oven at 37°C for 24 h the weight of the samples was recorded at regular time intervals. Evaporative water loss was calculated according to the formula in equation 6:

$$\text{Water loss}(\%) = W_t / W_0 \times 100 \quad (6)$$

Where W_t and W_0 are the weight after time 't' and initial weight after 24 h immersion time respectively.

2.7.5 Moisture content

The residual moisture content of wafers was determined by thermogravimetric analysis (TGA) using a Q5000-IR TGA instrument (TA Instruments, Crawley, UK). About 1.0 - 1.5mg of sample was accurately weighed, loaded and analyzed with dynamic heating from room temperature (~25°C) to 300°C at a heating rate of 10°C/min under inert nitrogen (N₂) gas at a flow rate of 50 mL/min. The percentage water content was calculated at 100°C using *TA Instruments Universal Analysis 2000* software program.

2.8 In-vitro drug dissolution and release profiles

The total content of CIP within the wafers was investigated before performing drug dissolution and release studies. This was done by hydrating the whole wafer in 10 ml of HPLC grade purified water at 37°C with stirring and left overnight to dissolve completely. The concentration of CIP in water was determined by HPLC and used to calculate the total amount of drug in water representing total drug content (assay) within the wafers. Calibration samples were prepared in triplicate in the concentration range from 1 to 100 µg/ml to plot standard curve ($y = 189.35x$; $R^2 = 0.9993$) for CIP and used to determine drug loading efficiency (%) of the selected formulations used for drug dissolution studies to calculate the percent drug released at each time point.

In vitro drug dissolution studies were performed by a diffusion cell (developed in-house at the University of Greenwich) containing SWF (pH 7.5) as dissolution medium but with no BSA to avoid blocking of the HPLC column. The diffusion cell was designed with a wire mesh on which the wafers were placed. The dissolution medium was poured just up to the wire mesh so that the lower surface of the wafers was always just touching the dissolution medium. The wafers (CA-50 µg, CA-100 µg and CA-250 µg) containing CIP were placed on the wire mesh and the whole assembly placed in a water bath maintained at a temperature of 37°C with constant stirring (600 rpm). At predetermined time intervals, 1 ml aliquots of dissolution medium were withdrawn and analyzed by HPLC, and also replaced with same amount of fresh warm medium (37°C) to keep a constant volume throughout the experiment. The dilution due to replacing fresh medium was considered while calculating the percentage drug release at each time point. The concentration of CIP released from the wafers was determined by applying the calibration curve and percentage drug release plotted against time. Triplicate determinations ($n = 3$) were made for each wafer selected. The kinetics of CIP release from the wafers were also determined by finding the best fit of the % release

against time data to Higuchi, Korsmeyer-Peppas, zero order and first order equations (see supplementary data).

2.9 HPLC analysis

The HPLC analysis was carried with an Agilent 1200 series HPLC (Agilent Technologies, UK) equipped with quaternary pump, degasser, auto sampler, and Agilent Chemstation[®] software package for running the instrument, data acquisition and data analysis. The analyte was separated at ambient temperature using a C18 analytical column. The UV detector was set at 280 nm. A two-solvent gradient elution was performed, solvent A 2% aqueous acetic acid solution and solvent B acetonitrile in the ratio of 70: 30. The flow rate was set at 1 ml/min and injection volume at 20 μ l.

2.10 In-vitro antimicrobial studies

Initially, minimum inhibitory concentration (MIC) of pure CIP and drug loaded (DL) wafers were determined by broth dilution method (see supplementary data). Further, antimicrobial activity of CIP loaded wafers was evaluated against *E. coli*, *S. aureus* and *P. aeruginosa* by turbidimetric and Kirby-Bauer disc diffusion methods.

2.10.1 Turbidimetric method

In this method, 10 ml of bacterial suspension (10^6 CFU/ml) was transferred into sterile test tubes each containing wafers obtained from gel with different concentrations of drug (0.0001-0.040% w/v). One of the tubes was left without sample and used as control. The tubes were incubated in an orbital shaking incubator at 37°C, and absorbance at 625 nm was measured at different time intervals (3, 6, 12 and 24 h) after treatment with each formulation. The experiment was carried out in triplicate ($n = 3$) against each organism (*E. coli*, *S. aureus* and *P. aeruginosa*).

2.10.2. Kirby-Bauer disk diffusion method

Bacterial inocula were prepared from 3-4 separate colonies of the tested organisms using a sterile inoculating loop. The colonies were suspended in 3 ml of MH growth medium and incubated overnight at 37°C. After overnight incubation, the turbidity of the bacterial suspension was adjusted to a 0.5 McFarland standard ($\sim 10^8$ CFU/ml) by diluting with the medium. Each suspension was further diluted to 10^6 CFU/ml (1 in 100) in a sterile tube. A

sterile swab was immersed into the tube and streaked on the surface of the entire MH plate three times with clockwise rotation. Circular dressings (diameter, 14-15 mm) were placed in the center of colonized agar plates and incubated at 37°C for 24 h, after which zone of inhibition (ZOI) in mm was measured using a digital Vernier caliper.

2.11 MTT (cell viability) assay

MTT assay on adult human primary epidermal keratinocytes (PCS-200-011, ATCC) was performed to evaluate the cytotoxicity of the dressings. The cells were cultured and maintained according to the ATCC recommended protocol (see supplementary data). Prior to testing, the dressings were sterilized with UV radiation overnight in a flow cabinet (NU-437-300E, NUAIRE). The sterilized samples were then immersed in 2.5 ml of complete growth medium and placed in the incubator (Heracell 150i CO₂ incubator, Thermo Scientific) at 37°C in 5% (v/v) CO₂ for 24 h. The extracts were collected through filtration using 0.2 µm filter. The concentration of the cells was optimized for the MTT assay (see supplementary data) and the cells were seeded into 96-well microtiter plates at optimum density (10000 cells/well). The plates were incubated at 37°C in 5% (v/v) CO₂ for 5 h to allow cells adherence. After that, media was removed and 100 µl of each sample extract was placed in triplicate into the wells. The plates were left in the incubator at 37 °C for up to 72 h. After each time point (24, 48 and 72 h), 10 µl of MTT reagent was added to each well including blank (medium only). The plates were returned to the incubator for 4 h or more until a purple precipitate was clearly visible under the inverted microscope (AE2000, Motic). The media was then removed and 100 µl of DMSO was added to all wells including controls. The plates were returned to the incubator for 30 min and the absorbance recorded at 492 nm by a microtiter plate reader (Multiskan FC, Thermo scientific) equipped with SkanIt for Multiskan FC 3.1 software (Thermo scientific). Every experiment was carried out in triplicates and repeated three times. The percentage of viable cells was calculated using equation 12.

$$\text{Cell viability (\%)} = \frac{A_t - A_b}{A_c - A_b} * 100 \quad (7)$$

Where A_t , A_b and A_c are the absorbance of tested samples, blank (medium only) and negative control (untreated cells) respectively.

Additionally, the effect of sample extracts on the cells morphology and adherence was recorded microscopically by FLoid® Cell Imaging Station. In this study, the untreated cells and Triton-X-100 (0.01% w/v) treated cells were used as negative (100% viable) and

positive controls respectively. Algisite Ag was chosen as a representative standard commercial sample for the MTT assay.

2.12 Statistical analysis

Statistical methods such as *t-test* and *ANOVA test* were performed by Excel to compare experimental values between BLK, DL wafers and Algisite Ag[®] and *p* values lower than 0.05 were considered significant.

3 Results and discussion

3.1. Formulation development

CA gels were prepared by the exchange of calcium ions with the monovalent sodium ions [43]. Among the different concentrations of CA gels prepared, 1% w/w was optimum in terms of ease of handling, viscous flow and pouring from the container when compared to 0.5%, 1.5% and 2 % w/w. **Fig. 1** shows the digital images of CA based wafers prepared by freeze-drying different gel concentrations (% w/w). After freeze-drying all wafers (1-2% w/w gels) appeared to be of uniform texture and thickness except wafer prepared from 0.5 % w/w gel. Wafers prepared from 0.5% w/w gel did not retain uniform structure because of low viscosity of the gel and subsequently low polymer network density. Subsequently, lyophilization of less viscous gel promoted premature ice crystallization during freezing and sublimation phases which resulted in flaky wafers.

3.2. Scanning electron microscopy (SEM)

SEM investigation showed that the BLK wafers were highly porous in morphology with large, uniform and circular shaped pores surrounded by a network of polymeric strands as shown in **Fig. 2**. It is reported that gels made from high α -L-guluronic acid alginates exhibit the highest porosity [52]. However, incorporation of CIP changed the uniformity of the pores in wafers. Increasing amount of CIP resulted in denser cores due to possible crosslinking between the drug and polymer during the freeze-drying process. In addition, **Fig. S1** shows SEM investigation of the both parts of the wafers. The bottom part of the wafer appears more porous in morphology than the top part. Such changes in surface characteristics has impact on other physicochemical properties such as hardness, swelling, adhesion, EWC, water absorption and WVTR [23,53] as discussed below.

3.3. *Texture analysis*

3.3.1. *Mechanical hardness*

The wafers ($n = 3$) were compressed at three different positions on the top and bottom sides to investigate the hardness (resistance to compressive deformation), and internal polymer and drug distribution. Hardness of all formulated wafers was tested to select optimum gel concentration for drug loading. Wafers prepared from 1% w/w gels showed excellent resistance to compression whereas wafers prepared from 1.5% and 2% w/w gels appeared very hard and brittle. On the other hand, wafers obtained from 0.5% w/w gel appeared to be very soft and flaky in nature which made them very difficult to handle. Therefore, the CIP was loaded into 1% w/w gels to obtain DL wafers.

Fig. 3 demonstrates the differences in hardness between the top and bottom sides of the wafers. The hardness of the top part of the wafers appeared higher than the lower part. This could be due to the higher polymer density on the upper part of the wafers than the bottom part. This is possible because in the shelf type freeze dryer used, the condenser is present in the lower part of the machine and freezing starts from bottom of the gel upwards. The higher polymer density leads to a more compact structure on the top surface of the wafer, which causes higher resistance to probe penetration. The difference in hardness between the sides of the wafers could also be attributed to differences in porosity [25]. As porosity increases, there is less force required to reach the required depth of penetration. Therefore, the lower surface of the wafers will be an ideal application site for applying to the wound bed as it will quickly absorb wound fluid due to higher porosity. Further, lower hardness will reduce the likelihood of damaging sensitive newly formed skin cells on a healing wound. However, to maintain hardness consistency of the wafers from container to container on a commercial scale, the containers must be flat bottom, with a wider diameter so that the gel and final wafer height (thickness) after freezing is not too big. Further, same amount of free flowing gel need to be poured in each well of the container. This way, the heat distribution within the frozen gel during primary drying will be more uniform between the top and bottom sides. This will yield thinner flat sheets similar to foam dressings and help produce consistent thickness and polymer density and subsequently will give consistent hardness. The advantage of wafer delivery dressing is that it can be produced in different sizes and shapes depending on the casting container and it can be delivered to the patients to suit the specific application area.

The BLK wafers showed significantly ($p = 0.0001$) higher hardness than the DL wafers (**Fig. 3**) and the hardness of the drug incorporated wafers decreased gradually with

increasing drug content. This could be explained by the fact that after loading drug, the availability of free polymer was reduced throughout the matrix, therefore the rigidity of polymeric matrix decreased and these results support the SEM observation (**Fig. 2**) below. In addition, the disturbance in porosity of DL wafers also resulted in a reduction of the hardness that might affect other physicochemical properties such as swelling, mucoadhesion, EWC, WVTR and drug release.

3.3.2. *In-vitro* adhesion studies

Stickiness, work of adhesion and cohesiveness are associated with the bond formation between the polymeric matrix and gelatin gel during the contact period.

Usually chronic wounds such as DFU contain highly viscous exudates [54], therefore in this study two different concentrations of BSA (2% w/w and 5% w/w) were used to represent thin and viscous wound exudate respectively. CA-BLK wafers showed similar stickiness (1.82 ± 0.06 N and 1.54 ± 0.47 N) in the presence of light SWF (2% w/w BSA) and viscous SWF (5% w/w BSA) respectively. DL wafers showed stickiness values around 0.55-0.26 N in the presence of both thin SWF (2% w/w BSA) and thick SWF (5% w/w BSA). It can be observed in **Fig. 4** that the CA-BLK wafer showed higher stickiness and WOA values than the DL dressings in both types of exudates. This could be due to the fact that incorporation of the drug into the wafers resulted in poor contact between the polymer chains and hence reduced adhesive properties. Stickiness also depends on the pore size distribution of the polymeric matrix. SEM images (**Fig. 2**) illustrated the disturbance in pore size distribution of DL wafers and also poorer hydration capacity possibly resulting in reduction in the stickiness.

3.4. *X-ray diffraction (XRD)*

Fig. 5a shows the XRD transmission diffractograms of pure CA and BLK wafers. Pure CA indicated amorphous structure but the wafer showed crystalline nature due to the presence of calcium carbonate (formed from the solvent used to dissolve the polymer) within the matrix with sharp peaks at 2θ of 23.06° , 29.42° , 31.53° , 35.97° , 39.42° , 43.16° , 47.53° and 48.5° . As shown in **Fig. 5b** pure CIP was highly crystalline in nature, showing several characteristic sharp peaks at 14.4° , 20.7° and 25.5° 2θ . Disappearance and / or decrease in intensity of these peaks in DL wafers (**Fig. 5c**) suggests that the drug was molecularly dispersed within the polymeric matrix and this is expected to impact upon the rate of drug release. Here, it is also important to note that the characteristic peaks of the dressings were slightly shifted to higher diffraction angle after loading drug indicating the possible

interaction of drug with the polymer. Moreover, the crystallinity of the dressings were decreased (data not shown) after loading drug indicating drug-polymer crosslinking and also confirmed by FTIR (see supplementary data).

3.5. Fluid (exudate) handling properties

3.5.1. Porosity

The highly porous structure of the wafers was obtained by freeze drying where, the gels were initially cooled (freezing) until pure ice crystals form and then sublimed (primary drying) from its frozen state under vacuum at low temperature (-25°C), leaving a highly porous microstructure [55]. Their highly porous structure permits transportation of gases, nutrients and regulatory factors to allow cell survival, proliferation and differentiation [56]. The porosity of BLK and DL dressings was determined by the solvent (ethanol) displacement method to avoid hydration of the polymer matrix and collapse of the pores.

As shown in **Table 1** wafers containing more than 0.0001% drug showed a high percentage porosity between $98.20 \pm 0.56 \%$ to $88.42 \pm 4.03\%$. This could be because the solvent penetrated well into the capillaries of wafers due to the roughness of the pore walls as shown in SEM images (**Fig. 2**). The highly porous dressings would play a vital role in carrying oxygen into the blood thus preventing ischemia in diabetic foot. All formulations showed the higher porosity than Algisite Ag[®] ($71.72 \pm 4.17 \%$). Therefore, the CIP loaded dressings will be expected to absorb more exudates than the commercial product. High porosity also has an effect on swelling, Aw, EWC, WVTR and drug release as described below.

3.5.2. Water holding (swelling, Aw and EWC) properties

The fluid handling ability of wafers plays a vital role in wound healing as it prevents maceration of healthy skin tissue in highly exuding DFUs. The swelling capacity of the dressings is closely related to porosity as greater number of pores accelerates higher swelling ability. However, it also depends on the shape, size and uniformity of the pores in the polymeric matrix as well as chemical interaction of polymer and drug with the swelling medium [23]. CA and CIP both contain a mixture of hydrophilic and hydrophobic functional groups such as hydroxyl, carboxyl, amine and carbonyl groups, which can improve the swelling properties. **Fig. 6** shows the swelling profiles of BLK and DL wafers in SWF.

The initial swelling ability of DL wafers (0.0001-0.005% CIP) was higher compared to BLK wafer with values ranging from $2055.30 \pm 192.65\%$ to $1476.90 \pm 95.69\%$ for the first 15 min. After that, the swelling capacities of all DL wafers gradually decreased up to 120 min, and

then remained steady for the rest of the study. The initial phase of fluid uptake can be explained as follows; the Ca^{2+} ions present in the mannuronate units of alginate are exchanged with Na^+ ions in SWF thus allowing faster ingress of fluid into the polymeric wafer matrix. Wafers containing more than 0.005% drug exhibited lower swelling capacity possibly due to losing their structural integrity resulting in easier polymer erosion in SWF during handling and blotting with the tissue paper. The steady water retention capability of the wafers occurred over an extended period thus indicating that the dressings can be used in highly exuding DFUs to prevent maceration whilst maintaining a moist wound environment. The swelling capacities of formulated wafers were compared with a commercial dressing, Algisite Ag (Smith & Nephew, UK). It was observed that the maximum swelling of Algisite Ag was about $816.16 \pm 28.58\%$ within 15 min ($p = 0.0008$), which was less than any CIP loaded wafers. It could be because the Algisite Ag[®] fiber mats appeared to be less porous (**Fig. S1**) in nature therefore permitted lower rate of water ingress.

The Aw and EWC capacity are the two important factors affecting the rapid absorption of exudates. As shown in **Table 1**, the BLK wafers exhibited the highest water absorption ($3373.54 \pm 169.85\%$) and EWC ($91.11 \pm 0.14\%$). After drug loading, the Aw and EWC gradually decreased with increasing drug content due to the increased cross-linking density of CIP with the polymer. Moreover, this could be due to the disturbance in pore size distribution as illustrated in SEM images (**Fig. 2**) after drug incorporation. The irregular pores within polymeric microstructure retards water ingress which resulted in decreasing water holding capacity into the matrix with increasing drug loading. Wafers containing 0.0001% CIP showed maximum water uptake at about $1858.27 \pm 65.38\%$ whilst the Aw of wafers containing 0.0005-0.005% CIP were insignificant ($p = 0.77$) ranging from 1583.21 ± 49.11 to $1519.85 \pm 127.61\%$. The water uptake capacities were dramatically decreased after loading more than 0.005% drug. This could be attributed to the dense pore network resulting in reduced void space to absorb water. The commercial product Algisite Ag[®] exhibited the lowest Aw ($580.61 \pm 95.30\%$) and EWC ($85.00 \pm 2.21\%$) amongst all formulations. This could be because Algisite Ag[®] is less porous in nature and suggests that the proposed CA

Table 1. The Porosity, moisture content, equilibrium water content, water absorption and water vapor transmission rate of different wafer formulations and the commercial silver dressing ($n = 3 \pm SD$).

| Sample | Porosity (%) | Moisture content (%) | EWC (%) | Water absorption (%) | WVTR (g/m²day⁻¹) |
|--------------------------------|---------------------|-----------------------------|----------------|-----------------------------|-----------------------------------------------|
| CA-BLK | 80.28 ± 1.45 | 13.28 ± 0.86 | 97.11 ± 0.14 | 3373.54 ± 169.85 | 2577.42 ± 261.98 |
| CA-CIP 0.0001% | 75.81 ± 3.96 | 16.78 ± 0.39 | 94.89 ± 0.17 | 1858.27 ± 65.38 | 3181.21 ± 48.75 |
| CA-CIP 0.0005% | 88.42 ± 4.03 | 16.74 ± 0.01 | 94.05 ± 0.17 | 1583.21 ± 49.11 | 3144.91 ± 24.72 |
| CA-CIP 0.0010% | 96.47 ± 2.24 | 16.71 ± 0.01 | 93.83 ± 0.14 | 1521.22 ± 36.77 | 3111.79 ± 16.79 |
| CA-CIP 0.0025% | 92.03 ± 1.00 | 16.56 ± 0.08 | 93.82 ± 0.09 | 1519.87 ± 23.94 | 3219.50 ± 59.54 |
| CA-CIP 0.005% | 98.20 ± 0.56 | 16.79 ± 0.03 | 93.79 ± 0.51 | 1519.85 ± 127.61 | 3445.66 ± 174.36 |
| CA-CIP 0.010% | 95.80 ± 3.06 | 17.01 ± 0.04 | 92.74 ± 0.24 | 1278.46 ± 45.34 | 3354.37 ± 11.73 |
| CA-CIP 0.025% | 94.79 ± 3.94 | 17.30 ± 0.04 | 91.57 ± 0.22 | 1086.66 ± 31.47 | 3499.23 ± 71.76 |
| CA-CIP 0.040% | 93.82 ± 2.81 | 16.83 ± 0.12 | 89.94 ± 0.78 | 900.27 ± 74.55 | 3413.97 ± 98.99 |
| Algisite Ag[®] | 71.72 ± 4.17 | - | 85.00 ± 2.21 | 580.61 ± 95.30 | 2995.97 ± 115.40 |

5 wafer developed in this study has great potential as an antimicrobial dressing for highly exuding DFUs.

3.5.3. *Water vapor transmission rate*

10 WVTR indicates the ability of dressings to absorb fluid and draw it out from the wound bed across the materials into the atmosphere. Wound dressings require an adequate level of moisture transmission to keep the wound area comfortable and promote the healing process. Dry wounds exhibit the most water loss thus decrease body temperature and rate of metabolism. Therefore, the wound dressing should reduce wound exudate significantly but provide adequate moisture content by maintaining a balance between water absorption and
15 transmission as well as humidity in the affected wound site [53]. Higher water vapor transmission rate promotes epithelization process of wound healing whilst lower WVTR delays the healing process by accumulating excess wound exudates [57] which leads to skin maceration, excoriation and microbial growth.

The rate of water loss was linear with time at regular intervals (data not shown). All
20 the wafers showed high WVTR (**Table 2**) that will be expected absorb and transmit exudates quickly. The high WVTR is attributed to the porosity of the dressings, resulting in the increase of voids with capillary adsorbed water. The DL wafers showed greater WVTR ranging from 3111.79 – 3499.23 g/m²day⁻¹ compared to the commercial Algisite Ag[®] (2995.97 ± 115.4 g/m²day⁻¹). It has been reported that patients with chronic leg ulcers
25 produce 5 g of exudate per 10 cm²/24 h [58], which was equivalent to 5000 g/m²/24 h. This suggests that CIP loaded dressings have the potential to absorb and take out about 62-70% fluid from chronic wound beds, however, this needs to be confirmed in an in vivo study.

3.5.4. *Evaporative water loss*

30 The evaporative water loss (EWL) of the wafers was recorded to determine the behavior of the dressings when exposed to air. As shown in **Fig. 7**, approximately 20% of water loss was observed in CA-BLK and the medicated wafers containing 0.0001-0.025% of the drug within 1 h whereas 0.040% DL wafer and Algisite Ag[®] showed 30% and 40% water loss respectively. However, the water loss of CIP loaded wafer increased up to approximately
35 87% within 7 h whereas Algisite Ag[®] had lost this amount within 3 h. After 7 h the loss of water was insignificant ($p = 0.76$) and all dressings retained 8-10% of water after 24 h. It indicates that the dressings will lose water when exposed to air. Thus, the dressings will be

effective in the early stage of highly exuding wounds such DFUs, as it enables the dressings to take up more exudates and edema fluid quickly from the wound bed into its matrix by an active upward-directed process [59].

3.5.5. *Moisture content*

Thermogravimetric analysis was used to determine the residual water content of wafers after freeze-drying. The moisture content of BLK wafer was about $13.28 \pm 0.86 \%$ whereas incorporation of CIP into the polymeric wafers resulted in significantly ($p = 0.004$) higher moisture content about $16.56 \pm 0.08 \%$ to $17.30 \pm 0.04 \%$ respectively. This seems to indicate that addition of CIP resulted in higher sorption characteristics. However, though, high residual water content into wafers is susceptible to microbial growth and also retards stability by accelerating crystallization of the drug upon storage [60], the levels are comparable to other reported studies [61-63]. Further, high moisture content of the wafers can maintain the wound and surrounding skin in an optimum state of hydration thus implies the dressings to functions efficiently under compression [64].

3.6. *In-vitro drug dissolution and release studies*

The percentage cumulative release profiles of CIP from the CA based wafers with different amounts of drug are shown in **Fig. 8**. Wafers loaded with 0.025% CIP appeared to produce the fastest release rate, releasing about $68.36 \pm 3.68\%$ of the total drug content within 5 min of dissolution. This means the burst release of the dressings can reach MBC for killing *E. coli*, *P. aeruginosa* and *S. aureus* within 5 min. However, wafers containing 0.005 and 0.010% CIP showed total release around $41.89 \pm 6.74\%$ and $20.91 \pm 6.32\%$ respectively in 5 min which is also high enough for killing *E. coli* and *P. aeruginosa*. The highest cumulative percent of CIP released in 6 h was about $59.40 \pm 0.64\%$, $74.39 \pm 3.59\%$ and $91.43 \pm 1.21\%$ from the wafers loaded with 0.005, 0.010 and 0.025% drug respectively. The dressings containing higher amount of CIP appeared to release the drug more rapidly. This could be due to disturbance in pore distribution within the wafers. The irregular pore size allows quick hydration and therefore faster rate of drug release [65]. Though the initial fast release is over between 1 and 3 hours, the sustained amounts of CIP from the dressings up to 6 h can prevent re-infection as well as the need for frequent dressing change.

The drug release from wafers was the best fitted ($R^2 = 0.86-0.95$) to Korsmeyer-Peppas mechanism compared to other equations (**Table S1**) as noted previously [62, 66, 67]. Therefore, drug released through the polymeric matrix is either by Fickian or non-Fickian

diffusion which is the combination of both diffusion and erosion controlled release mechanism. Wafers containing 0.005 and 0.025% CIP showed drug release by Fickian diffusion as their n values were less than 0.45. The wafer containing 0.010% CIP showed non-Fickian diffusion (see details in supplementary section).

3.7. *In-vitro antimicrobial study*

In this study, the MIC and MBC (99.9% inhibition) of pure CIP for *E. coli*, *S. aureus* and *P. aeruginosa* were recorded as 0.06, 0.5 and 0.125 µg/ml and 0.25, 4, and 0.5 respectively. On the other hand, the MIC of DL wafers was 0.0001% CIP for *E. coli* and 0.0005% CIP for *S. aureus* and *P. aeruginosa*. Moreover, the wafers with 0.0010 % CIP exhibited MBC for *E. coli* and *P. aeruginosa*; followed by 0.005% CIP for *S. aureus* (see details in the supplementary section).

Antimicrobial activity of CIP loaded wafers and Algisite Ag[®] were assayed by turbidimetric and Kirby-Bauer disk diffusion method. In turbidity assay, optical densities (OD) of the samples were measured at 625 nm at different time intervals and the turbidity was also analyzed visually as shown in **Fig. S3 D-F**. The clear solutions of bacterial suspension confirmed the effectiveness of the released antibiotic in eradicating the bacterial load. A significant difference ($p=0.001$) in absorbance values was detected between *E. coli*, *S. aureus* and *P. aeruginosa* incubated with BLK and antibiotic loaded wafers (**Fig. S5 a-c**). BLK wafers did not show any antibacterial effects, which was also confirmed by the ZOI assay (**Fig. S6**). However, the extent of effectiveness of the antibiotic indicated quick release of the drug from the polymeric matrix. The OD values of the control and CA-BLK gradually increased with time, whereas the values remained below 0.5 in the case of DL wafers during the incubation period. The results suggest that the rate of bacterial inhibition was rapid for the DL dressings and this was further verified by counting number of viable cells at regular time intervals during incubation (**Fig. S7**). **Fig. S7** revealed that *E. coli* (**a**) and *P. aeruginosa* (**c**) were completely eradicated within 1.5 h of incubation with the dressings (CA-CIP 0.005%, CA-CIP 0.010% and CA-CIP 0.025%) whilst it took 24 h to kill *S. aureus* (**b**) completely.

100

Table 2. Zone of inhibition (ZOI) of CIP loaded wafers and Algiste Ag[®] against *E. coli*, *S. aureus* and *P. aeruginosa*.

| Sample | <i>E. coli</i> ZOI (mm) | <i>S. aureus</i> ZOI (mm) | <i>P. aeruginosa</i> ZOI (mm) |
|-------------------------|----------------------------|------------------------------|----------------------------------|
| CA-BLK | 0.00 ± 0.00 | 0.00 ± 0.00 | 0.00 ± 0.00 |
| CA-CIP 0.0001% | 29.67 ± 0.47 | 20.00 ± 0.82 | 31.00 ± 0.82 |
| CA-CIP 0.0005% | 33.83 ± 0.24 | 25.67 ± 0.47 | 35.83 ± 0.43 |
| CA-CIP 0.0010% | 34.83 ± 0.65 | 30.33 ± 0.94 | 36.83 ± 0.24 |
| CA-CIP 0.0025% | 37.17 ± 0.11 | 31.67 ± 0.23 | 37.17 ± 0.39 |
| CA-CIP 0.005% | 40.47 ± 0.41 | 33.07 ± 0.09 | 37.40 ± 0.45 |
| CA-CIP 0.010% | 41.43 ± 0.49 | 33.37 ± 0.29 | 38.97 ± 0.94 |
| CA-CIP 0.025% | 43.43 ± 0.34 | 34.67 ± 0.47 | 40.00 ± 0.08 |
| CA-CIP 0.040% | 45.07 ± 0.40 | 36.23 ± 0.34 | 41.33 ± 0.62 |
| Algiste Ag [®] | 0.00 ± 0.00 | 33.33 ± 0.49 | 0.00 ± 0.00 |

105 **Fig. S6** and **Table 2** show the zones and diameter of zone of inhibition (ZOI) respectively of the tested bacteria in the presence of BLK wafers, DL wafers and Algiste Ag[®]. As shown in **Fig. S6** CA-BLK wafer did not show any zone of inhibition against *E. coli*, *S. aureus* and *P. aeruginosa*. This result confirmed that the polymer has no antibacterial activity alone. However, clear zones of inhibition were observed in DL wafers for both

110 Gram-positive and Gram-negative bacteria. In addition, the mean diameters (mm) of ZOI for all three microorganisms increased with increasing drug content within the wafers. As recorded in **Table 2** for *E. coli* the mean diameter of ZOI of the wafers with 0.0001% (MIC) and 0.0010% (MBC) CIP was around 29.67 ± 0.47 mm and 34.83 ± 0.65 mm respectively. The largest zone (45.07 ± 0.40 mm) was observed against *E. coli* for the wafer containing

115 0.040% CIP. In the case of *S. aureus* and *P. aeruginosa*, the ZOI of 0.0005% CIP loaded wafer (MIC for *S. aureus* and *P. aeruginosa*), reached 25.67 ± 0.47 mm and 35.83 ± 0.43 mm. Moreover, the ZOI for wafers loaded with 0.005% (MBC for *S. aureus*) and 0.0010% (MBC for *P. aeruginosa*) CIP were recorded around 33.07 ± 0.09 mm and 36.83 ± 0.24 mm respectively. Overall higher ZOIs as well as maximum killing ability at low concentration

120 confirmed that CIP is more active against *E. coli* and *P. aeruginosa* than *S. aureus*. No bactericidal activity was detected for Algiste Ag against *E. coli* and *P. aeruginosa* except *S. aureus* as illustrated in **Fig. S6** with a ZOI value about 33.33 ± 0.49 mm against *S. aureus*.

This implies that CIP loaded wafers have better antimicrobial activity than the commercial product.

125

3.8. *In-vitro cell viability studies*

Biocompatibility is a vital requirement recommended by the International Organization for Standardization (ISO) for the safe use of medical devices and materials. Cytotoxicity test is an integral part of biological evaluation, which determines the prevalence of toxic effect and also determines the presence of positive influence in terms of biofunctionality that promotes wound healing [68]. The biocompatibility of DL dressings was evaluated in *in vitro* cultures of human primary epidermal keratinocytes (PEK) cell line for 24, 48 and 72h respectively. Keratinocytes are the main cellular component of human skin and therefore, selected as an *in-vitro* model for MTT assay. Moreover, PEK has been investigated as a useful model for testing *in vitro* wound healing activity in the literature [53,69,70]. The colorimetric MTT assay is based on enzymatic conversion in which MTT is converted to purple formazan by the action of dehydrogenase enzymes [71]. In this study, the untreated cells and Triton-X-100 (0.01% w/v) treated cells were used as negative (100% viable) and positive controls respectively. Algisite Ag was chosen as a representative standard commercial sample for the MTT assay. The positive control Triton-X-100 showed more than 100% cytotoxicity and resulted in a significant reduction in cell viability to values below 0% after 72 h treatment. The CIP loaded wafers were found to be highly biocompatible with less influence on the viability of the keratinocytes as shown in **Fig. 9**. Microscopic observations (**Fig. S8**) also revealed the biocompatibility of the dressings to the cells. Wafers containing 0.0001-0.025% CIP exhibited more than 85% cell viability whereas 0.040% drug loaded wafer and Algisite Ag[®] showed just below 80% cell viability over the 72 h incubation period. A time dependent toxicity was also observed after treatment of PEK cells with the extracts of CIP loaded wafers. According to the ISO guideline (DIN EN ISO 10993-5) the *in vitro* cell viability of medical devices and materials after exposure should be $\geq 70\%$ to be considered as non-cytotoxic [69]. Therefore, according to these guidelines all DL dressings exhibited acceptable cell viabilities of PEK. Moreover, dressings containing CIP have been reported safe to fibroblasts [37]. However, pure CIP has been reported to exhibit time dependent cytotoxicity on fibroblast cell lines at concentrations of 0.129 and 0.194 mM, following 48 and 72 h of exposure respectively [72]. On the other hand, none of the literature reviewed the cytotoxicity of CIP loaded dressings on PEK cell lines. Therefore, the present

155

work reveals that CIP loaded lyophilized wafers are non-toxic to PEK and appear to be safe dressings for healing of DFUs.

4 Conclusions

160 A fluoroquinolone-polymer composite to be applied as a dressing in DFUs was formulated and characterised in terms of functional physicochemical properties, antimicrobial activity and cell viability. The uniform distribution of CIP within the CA based polymeric matrix was confirmed by SEM, FTIR and XRD. The evaluation of swelling, porosity, moisture content, water absorption and EWC showed high capacity of handling wound exudates which can
165 prevent maceration of healthy skin cells in DFU. In addition, WVTR (3111.79 – 3499.23 $\text{g/m}^2\text{day}^{-1}$) and EWL (87% within 7 h) study reflected optimal conditions for maintaining moist environment, which is necessary for wound healing. The rapid eradication of three common infection causative bacteria; *E. coli*, *S. aureus* and *P. aeruginosa* was attributed to initial burst release of drug. The lyophilized wafers showed acceptable cell viability above
170 70% with respect to ISO standard. By considering the data of antimicrobial and cell viability studies, it will be a potential dressing for patients with DFUs infected with drug resistant bacteria. In addition, the CIP loaded wafers showed better fluid handling capacity, bacterial inhibition as well as cell survival (MTT assay) than Algisite Ag[®] commercial dressing. Therefore, the CIP loaded wafers will be potentially a better dressing than the commercial
175 product for DFUs. Studies of cell migration and attachment as well as *in vivo* animal testing are needed to elucidate the wound healing action of the lyophilized dressings.

Acknowledgments:

The authors will like to thank Samantha Lewis for her help with microbial analyses, Andrew
180 Hurt for help with XRD and SEM analyses.

Funding:

This research did not receive any specific grant from funding agencies in the public, commercial, or not-for-profit sectors.

185

Conflicts:

The authors report no conflicts of interest

190 **References**

1. Boateng J, Catanzano O. Advanced Therapeutic Dressings for Effective Wound Healing - A Review. *J. Pharm. Sci.* 2015;104:3653–80.
2. Sarheed O, Ahmed A, Shouqair D, Boateng JS. Antimicrobial Dressings for Improving Wound Healing. In: Alexandrescu V, editor. *Wound Healing - New insights into Ancient Challenges*. InTech (online); 2016. pp. 377-402. <https://www.intechopen.com/books/wound-healing-new-insights-into-ancient-challenges/antimicrobial-dressings-for-improving-wound-healing>. Accessed 4 Dec 2016.
3. Guo S, Dipietro LA. Factors affecting wound healing. *J. Dent. Res.* 2010;89:219–29.
4. Singh N, Armstrong DG, Lipsky BA. Preventing foot ulcers in patients with diabetes. *JAMA.* 2005;293:217–28.
5. Ravichandran P, Chitti SP. Antimicrobial Dressing for Diabetic Foot Ulcer Colonized with MRSA. *Online J. Biol. Sci.* 2015;15:282–91.
6. Kerr M. Diabetic Foot Care in England: an Economic Study. *Insight Heal Econ.* 2017;(January):1-52. [https://www.diabetes.org.uk/Upload/Shared practice/Diabetic footcare in England, An economic case study \(January 2017\).pdf](https://www.diabetes.org.uk/Upload/Shared%20practice/Diabetic%20footcare%20in%20England,%20An%20economic%20case%20study%20(January%202017).pdf). Accessed 5 Oct, 2017.
7. Alavi A, Sibbald RG, Mayer D, Goodman L, Botros M, Armstrong DG, et al. Diabetic foot ulcers: Part I. Pathophysiology and prevention. *J. Am. Acad. Dermatol.* 2014; doi:10.1016/j.jaad.2013.06.055.
8. Edmonds M. The treatment of diabetic foot infections: Focus on ertapenem. *Vasc. Health Risk Manag.* 2009;5:949–63.
9. Chiță T, Muntean D, Badițoiu L, Timar B, Moldovan R, Timar R, et al. Staphylococcus aureus strains isolated from diabetic foot ulcers. Identification of the antibiotic resistant phenotypes. *Rom. J. Diabetes Nutr. Metab. Dis.* 2013;20:389–93.
10. Zubair M, Malik A, Ahmad J. Clinico-microbiological study and antimicrobial drug resistance profile of diabetic foot infections in North India. *Foot (Edinb).* 2011;21:6–14.
11. O’Loughlin A, McIntosh C, Dinneen SF, O’Brien T. Review paper: basic concepts to novel therapies: a review of the diabetic foot. *Int. J. Low. Extrem. Wounds.* 2010;9:90–102.
12. Hilton JR, Williams DT, Beuker B, Miller DR, Harding KG. Wound dressings in diabetic foot disease. *Clin. Infect. Dis.* 2004;39 Suppl 2:100-3.
13. Yazdanpanah L, Nasiri M, Adarvishi S. Literature review on the management of diabetic foot ulcer. *World J. Diabetes.* 2015;6:37–53.
14. Boateng JS, Matthews KH, Stevens HNE, Eccleston GM. Wound healing dressings and drug delivery systems: A review. *J. Pharm. Sci.* 2008;9:2892–923.

15. Chang KW, Alsagoff S, Ong KT, Sim PH. Pressure ulcers--randomised controlled trial comparing hydrocolloid and saline gauze dressings. *Med. J. Malaysia.* 1998;53:428-31.
16. File TM, Tan JS. Amdinocillin plus cefoxitin versus cefoxitin alone in therapy of mixed soft tissue infections (including diabetic foot infections). *Am. J. Med.* 1983;75:100-5.
17. Fierer J, Daniel D. The fetid foot: Lower-extremity infections in patients with diabetes mellitus. *Rev. Infect. Dis.* 1979;1:210-7.
18. Lipsky BA, Pecoraro RE, Larson SA, Hanley ME, Ahroni JH. Outpatient management of uncomplicated lower-extremity infections in diabetic patients. *Arch. Intern. Med.* 1990;150:790-7.
19. Lipsky BA, Baker PD, Landon GC, Fernau R. Antibiotic therapy for diabetic foot infections: comparison of two parenteral-to-oral regimens. *Clin. Infect. Dis.* 1997;24:643-8.
20. Lipsky BA, Stoutenburgh U. Daptomycin for treating infected diabetic foot ulcers: Evidence from a randomized, controlled trial comparing daptomycin with vancomycin or semi-synthetic penicillins for complicated skin and skin-structure infections. *J. Antimicrob. Chemother.* 2005;55:240-5.
21. Boateng J, Burgos-Amador R, Okeke O, Pawar H. Composite alginate and gelatin based bio-polymeric wafers containing silver sulfadiazine for wound healing. *Int. J. Biol. Macromol.* 2015;79:63-71.
22. Labovitiadi O, Lamb AJ, Matthews KH. In vitro efficacy of antimicrobial wafers against methicillin-resistant *Staphylococcus aureus*. *Ther. Deliv.* 2012;3:443-55.
23. Pawar H V., Boateng JS, Ayensu I, Tetteh J. Multifunctional medicated lyophilised wafer dressing for effective chronic wound healing. *J. Pharm. Sci.* 2014;103:1720-33.
24. Boateng JS, Pawar H V, Tetteh J. Evaluation of in vitro wound adhesion characteristics of composite film and wafer based dressings using texture analysis and FTIR spectroscopy: a chemometrics factor analysis approach. *RSC Adv.* 2015;5:107064-75.
25. Boateng JS, Auffret AD, Matthews KH, Humphrey MJ, Stevens HNE, Eccleston GM. Characterisation of freeze-dried wafers and solvent evaporated films as potential drug delivery systems to mucosal surfaces. *Int. J. Pharm.* 2010;389:24-31.
26. Catanzano O, Docking R, Schofield P, Boateng J. Advanced multi-targeted composite biomaterial dressing for pain and infection control in chronic leg ulcers. *Carbohydr. Polym.* 2017;172:40-8.
27. Rezvanian M, Tan CK, Ng SF. Simvastatin-loaded lyophilized wafers as a potential dressing for chronic wounds. *Drug Dev. Ind. Pharm.* 2016;42:2055-62.
28. Sarheed O, Abdul Rasool BK, Abu-Gharbieh E, Aziz US. An Investigation and

- 260 Characterization on Alginate Hydrogel Dressing Loaded with Metronidazole Prepared by
Combined Inotropic Gelation and Freeze-Thawing Cycles for Controlled Release. *AAPS
PharmSciTech.* 2015;16:601–9.
29. Nagesh G, Santosh J, Audumbar M, Manojkumar P. A review on recent trends in oral
drug delivery- lyophilized wafer technology. *Int J. Res. Pharm and Pharm. Sci.* 2016;1:5-9.
30. Puoci F, Piangiolino C, Givigliano F, Parisi OI, Cassano R, Trombino S, et al.
Ciprofloxacin-collagen conjugate in the wound healing treatment. *J. Funct. Biomater.*
265 2012;3:361–71.
31. Jannesari M, Varshosaz J, Morshed M, Zamani M. Composite poly(vinyl
alcohol)/poly(vinyl acetate) electrospun nanofibrous mats as a novel wound dressing matrix
for controlled release of drugs. *Int. J. Nanomedicine.* 2011;6:993–1003.
32. Kataria K, Gupta A, Rath G, Mathur RB, Dhakate SR. In vivo wound healing
270 performance of drug loaded electrospun composite nanofibers transdermal patch. *Int. J.
Pharm.* 2014;469:102–10.
33. Öztürk E, Agalar C, Keçeci K, Denkbaş EB. Preparation and characterization of
ciprofloxacin-loaded alginate/chitosan sponge as a wound dressing material. *J. Appl. Polym.
Sci.* 2006;101:1602–9.
- 275 34. Roy DC, Tomblyn S, Burmeister DM, Wrice NL, Becerra SC, Burnett LR, et al.
Ciprofloxacin-Loaded Keratin Hydrogels Prevent *Pseudomonas aeruginosa* Infection and
Support Healing in a Porcine Full-Thickness Excisional Wound. *Adv. Wound Care.*
2015;4:457–68.
- 280 35. TVL HB, Vidyavathi M, K K, Sastry T, RV S kumar, Hima BT, et al. Preparation and
evaluation of ciprofloxacin loaded chitosan-gelatin composite films for wound healing
activity. *Int. J. Drug Deliv.* 2010;2:173–82.
36. Shi Y, Truong VX, Kulkarni K, Qu Y, Simon GP, Boyd RL, et al. Light-Triggered
Release of Ciprofloxacin from an in situ Forming Click Hydrogel for Antibacterial Wound
Dressings. *J. Mater. Chem. B. Royal Society of Chemistry;* 2015;3:3–6.
- 285 37. Unnithan AR, Barakat NAM, Tirupathi Pichiah PB, Gnanasekaran G, Nirmala R, Cha
YS, et al. Wound-dressing materials with antibacterial activity from electrospun
polyurethane-dextran nanofiber mats containing ciprofloxacin HCl. *Carbohydr. Polym.*
2012;90:1786–93.
38. Lipsky BA, Holroyd KJ, Zasloff M. Topical versus systemic antimicrobial therapy for
290 treating mildly infected diabetic foot ulcers: a randomized, controlled, double-blinded,
multicenter trial of pexiganan cream. *Clin. Infect. Dis.* 2008;47:1537–45.

39. Beberok A, Buszman E, Wrześniok D, Otręba M, Trzcionka J. Interaction between ciprofloxacin and melanin: The effect on proliferation and melanization in melanocytes. *Eur. J. Pharmacol.* 2011;669:32–7.
- 295 40. Malafaya PB, Silva GA, Reis RL. Natural-origin polymers as carriers and scaffolds for biomolecules and cell delivery in tissue engineering applications. *Adv. Drug Deliv. Rev.* 2007;59:207–33.
41. Daemi H, Barikani M. Synthesis and characterization of calcium alginate nanoparticles, sodium homopolymannuronate salt and its calcium nanoparticles. *Sci. Iran.* 2012;19:2023–8.
- 300 42. Taskin AK, Yasar M, Ozaydin I, Kaya B, Bat O, Ankarali S, et al. The hemostatic effect of calcium alginate in experimental splenic injury model. *Ulus. Travma Acil Cerrahi Derg.* 2013;19:195–9.
43. Shilpa A, Agrawal SS, Ray AR. Controlled Delivery of Drugs from Alginate Matrix. *J. Macromol. Sci. Part C Polym. Rev.* 2003;43:187–221.
- 305 44. Lloyd LL, Kennedy JF, Methacanon P, Paterson M, Knill CJ. Carbohydrate polymers as wound management aids. *Carbohydr. Polym.* 1998;37:315–22.
45. Tarun K, Gobi N. Calcium alginate/PVA blended nano fibre matrix for wound dressing. *Indian J. Fibre Text. Res.* 2012;37:127–32.
46. Moura LIF, Dias AMA, Carvalho E, de Sousa HC. Recent advances on the development
310 of wound dressings for diabetic foot ulcer treatment—A review. *Acta Biomater.* 2013;9:7093–114.
47. Lansdown ABG, Lansdown ABG. A Pharmacological and Toxicological Profile of Silver as an Antimicrobial Agent in Medical Devices. *Adv. Pharmacol. Sci.* 2010;2010:1–16.
48. Hiro ME, Pierpont YN, Ko F, Wright TE, Robson MC, Payne WG. Comparative
315 evaluation of silver-containing antimicrobial dressings on in vitro and in vivo processes of wound healing. *Eplasty.* 2012;12:409-19.
49. Burd A, Kwok CH, Hung SC, Chan HS, Gu H, Lam WK, et al. A comparative study of the cytotoxicity of silver-based dressings in monolayer cell, tissue explant, and animal models. *Wound Repair Regen.* 2007;15:94-104.
- 320 50. Bergin S, Wraith P. Silver based wound dressings and topical agents for treating diabetic foot ulcers. *Cochrane Database Syst. Rev.* 2006; doi:10.1002/14651858.CD005082.pub2.
51. Han J, Zhou Z, Yin R, Yang D, Nie J. Alginate-chitosan/hydroxyapatite polyelectrolyte complex porous scaffolds: Preparation and characterization. *Int. J. Biol. Macromol.* 2010;46:199–205.
- 325 52. Gombotz WR, Wee S. Protein release from alginate matrixes. *Adv. Drug Deliv. Rev.*

1998;31:267–85.

53. Kim IY, Yoo MK, Seo JH, Park SS, Na HS, Lee HC, et al. Evaluation of semi-interpenetrating polymer networks composed of chitosan and poloxamer for wound dressing application. *Int. J. Pharm.* 2007;341:35–43.

330 54. Speak K. Management of highly exuding diabetic foot ulcers. *Diabet. Foot Canada.* 2014;2:28–33.

55. Nireesha G, Divya L, Sowmya C, Venkateshan N, Niranjan Babu M, Lavakumar V. Lyophilization/Freeze Drying -An Review. *Ijntps.* 2013;3:87–98.

335 56. Dhandayuthapani B, Yoshida Y, Maekawa T, Kumar DS. Polymeric scaffolds in tissue engineering application: A review. *Int. J. Polym. Sci.* 2011; doi.org/10.1155/2011/290602.

57. Xu R, Xia H, He W, Li Z, Zhao J, Liu B, et al. Controlled water vapor transmission rate promotes wound-healing via wound re-epithelialization and contraction enhancement. *Sci. Rep.* Nature Publishing Group; 2016; doi.org/10.1038/srep24596.

340 58. Thomas S, Hay P. Fluid handling properties of hydrogel dressings. *Ostomy. Wound. Manage.* 1995;41:54–9.

59. Balakrishnan B, Mohanty M, Umashankar PR, Jayakrishnan A. Evaluation of an in situ forming hydrogel wound dressing based on oxidized alginate and gelatin. *Biomaterials.* 2005;26:6335–42.

345 60. Kianfar F, Antonijevic M, Chowdhry B, Boateng JS. Lyophilized wafers comprising carrageenan and pluronic acid for buccal drug delivery using model soluble and insoluble drugs. *Colloids Surfaces B Biointerfaces.* 2013;103:99–106.

61. Kianfar F, Ayensu I, Boateng JS. Development and physico-mechanical characterization of carrageenan and poloxamer-based lyophilized matrix as a potential buccal drug delivery system. *Drug Dev. Ind. Pharm.* 2013;9045:1–9.

350 62. Momoh FU, Boateng JS, Richardson SCW, Chowdhry BZ, Mitchell JC. International Journal of Biological Macromolecules Development and functional characterization of alginate dressing as potential protein delivery system for wound healing. *Int. J. Biol. Macromol.* 2015;81:137–50.

355 63. Kianfar F, Chowdhry BZ, Antonijevic MD, Boateng JS. Novel films for drug delivery via the buccal mucosa using model soluble and insoluble drugs. 2012;38:1207–20.

64. Thomas S. The role of dressings in the treatment of moisture-related skin damage. *World Wide Wounds.* 2008. <http://www.worldwidewounds.com/2008/march/Thomas/Maceration-and-the-role-of-dressings.html>. Accessed 14 Jan 2017.

65. Ayensu I, Mitchell JC, Boateng JS. Development and physico-mechanical

- 360 characterisation of lyophilised chitosan wafers as potential protein drug delivery systems via
the buccal mucosa. *Colloids Surfaces B Biointerfaces*. 2012;91:258–65.
66. Boateng JS, Matthews KH, Auffret AD, Humphrey MJ, Stevens HN, Eccleston GM. In
vitro drug release studies of polymeric freeze-dried wafers and solvent-cast films using
paracetamol as a model soluble drug. *Int. J. Pharm.* 2009;378:66–72.
- 365 67. Boateng JS, Matthews KH, Auffret AD, Humphrey MJ, Eccleston GM, Stevens HN.
Comparison of the in vitro release characteristics of mucosal freeze-dried wafers and solvent-
cast films containing an insoluble drug. *Drug Dev. Ind. Pharm.* 2012;38:47–54.
68. Wiegand C, Hipler U-C. Methods for the measurement of cell and tissue compatibility
including tissue regeneration processes. *GMS Krankenhaushygiene Interdiszip.* 2008;3:1–9.
- 370 69. Moritz S, Wiegand C, Wesarg F, Hessler N, Muller FA, Kralisch D, et al. Active wound
dressings based on bacterial nanocellulose as drug delivery system for octenidine. *Int. J.*
Pharm. 2014;471:45-55.
70. Moritz S, Wiegand C, Wesarg F, Hessler N, Muller FA, Kralisch D, et al. Active wound
dressings based on bacterial nanocellulose as drug delivery system for octenidine. *Int. J.*
375 *Pharm.* 2014;471:45-55.
71. Zhou C, Heath DE, Sharif ARM, Rayatpisheh S, Oh BHL, Rong X, et al. High water
content hydrogel with super high refractive index. *Macromol. Biosci.* 2013;13:1485–91.
72. Gurbay A, Garrel C, Osman M, Richard MJ, Favier A, Hincal F. Cytotoxicity in
ciprofloxacin-treated human fibroblast cells and protection by vitamin E. *Hum. Exp. Toxicol.*
380 2002;21:635–41.

385

Figure legends

390 Figure 1 Digital images of CA wafers prepared from gels of different concentrations based on total polymer weight

Figure 2 SEM images of BLK and CIP loaded wafers captured at x200 magnification

395 Figure 3 Hardness profiles of formulated wafers ($n = 3$) prepared from 1% w/w gels, compressed at three different places on both sides of the dressing showing effect of drug loading

Figure 4 Adhesive profiles of CIP loaded wafers in the presence of (a) thin SWF containing 400 2% (w/w) BSA and (b) viscous SWF containing 5% (w/w) BSA

Figure 5 XRD patterns of (a) pure polymer and BLK wafer, (b) pure drug and (c) drug loaded wafers

405 Figure 6 Swelling behavior of the different CA based dressings tested

Figure 7 Evaporative water loss from Algisite Ag[®], BLK and DL wafers

Figure 8 Cumulative percentage drug release profiles of optimized CIP loaded wafers 410

Figure 9 Cell viability of human primary epidermal keratinocytes after expositions to the extracts of CIP loaded wafers and fiber mat, Algisite Ag[®] for 24, 48 and 72 h (mean \pm SD, $n = 9$)

415

420

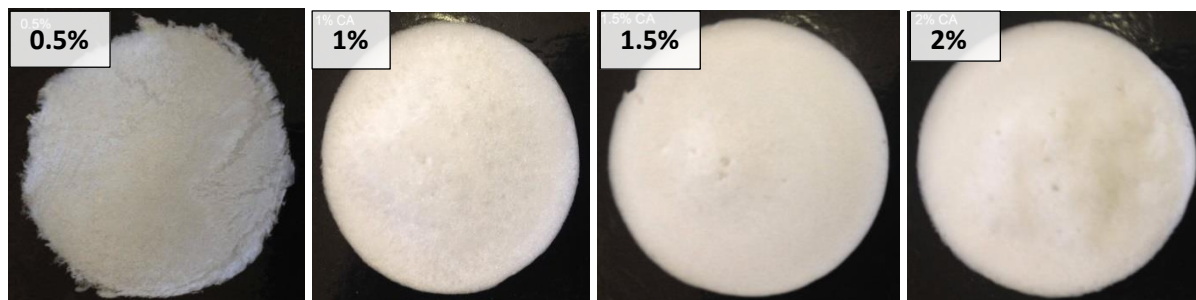
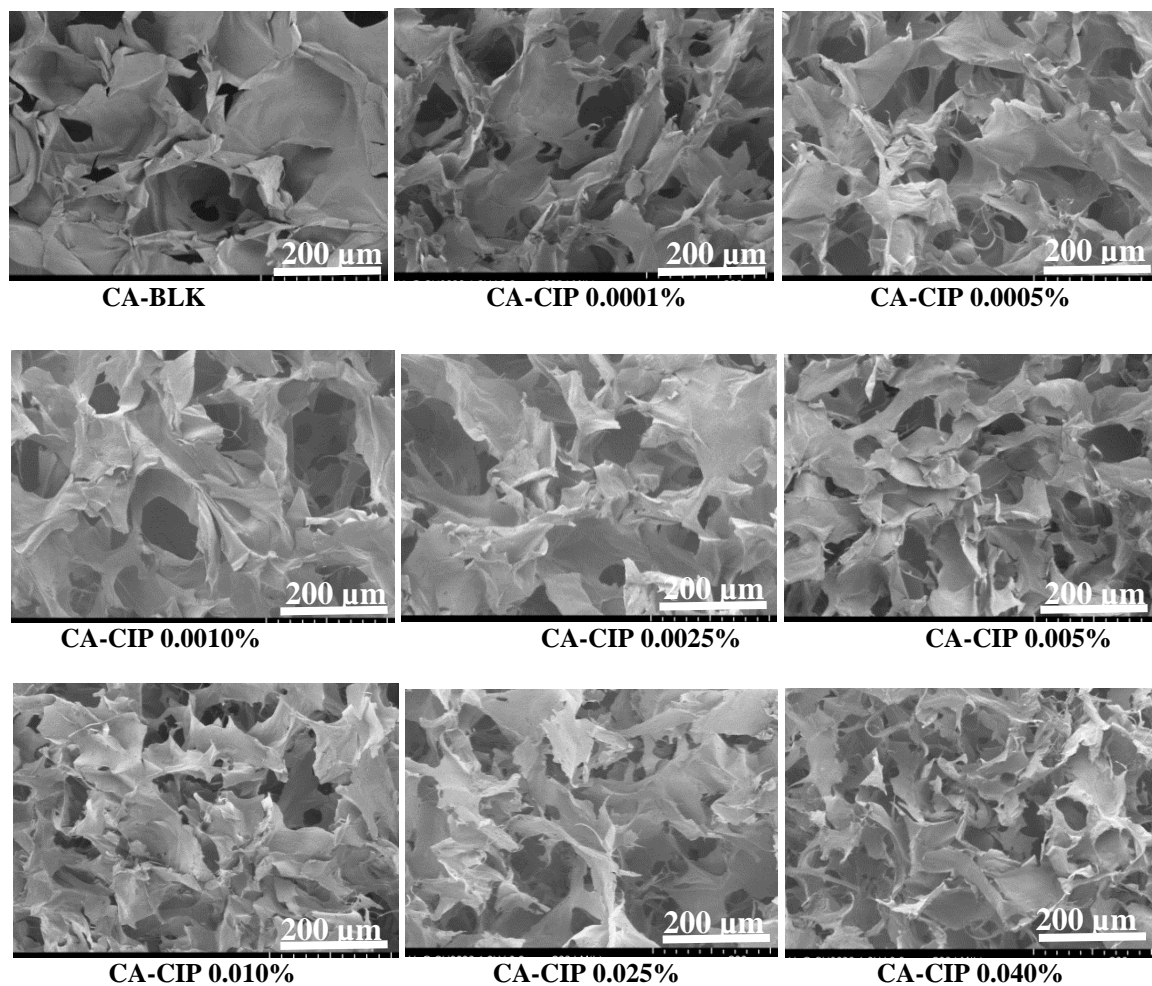


Figure 1 Digital images of CA wafers prepared from gels of different concentrations based on total polymer weight.

435



440

445

Figure 2 SEM images of BLK and CIP loaded wafers captured at x200 magnification.

450

455

460

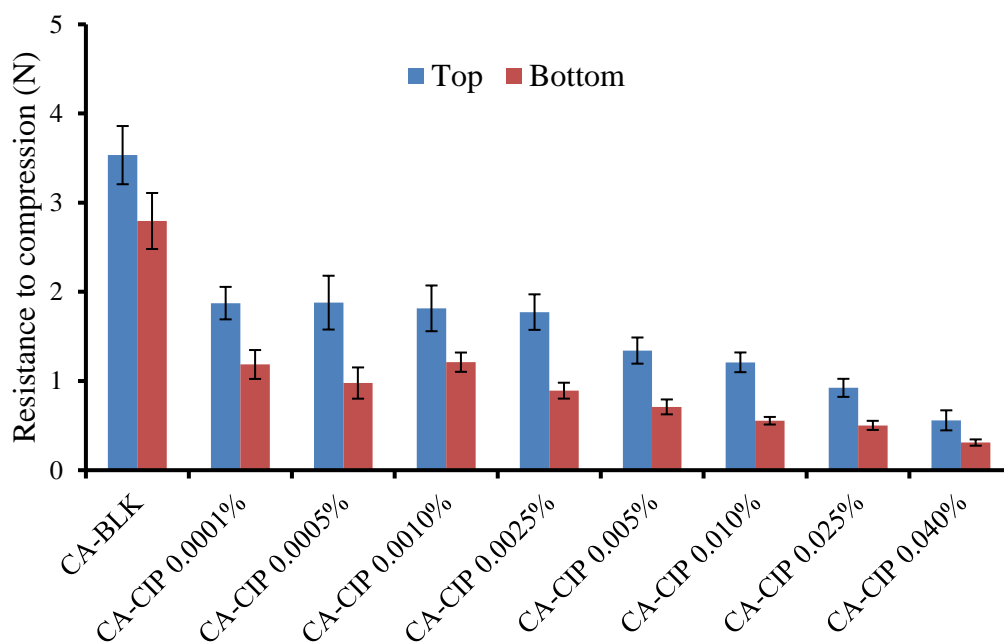
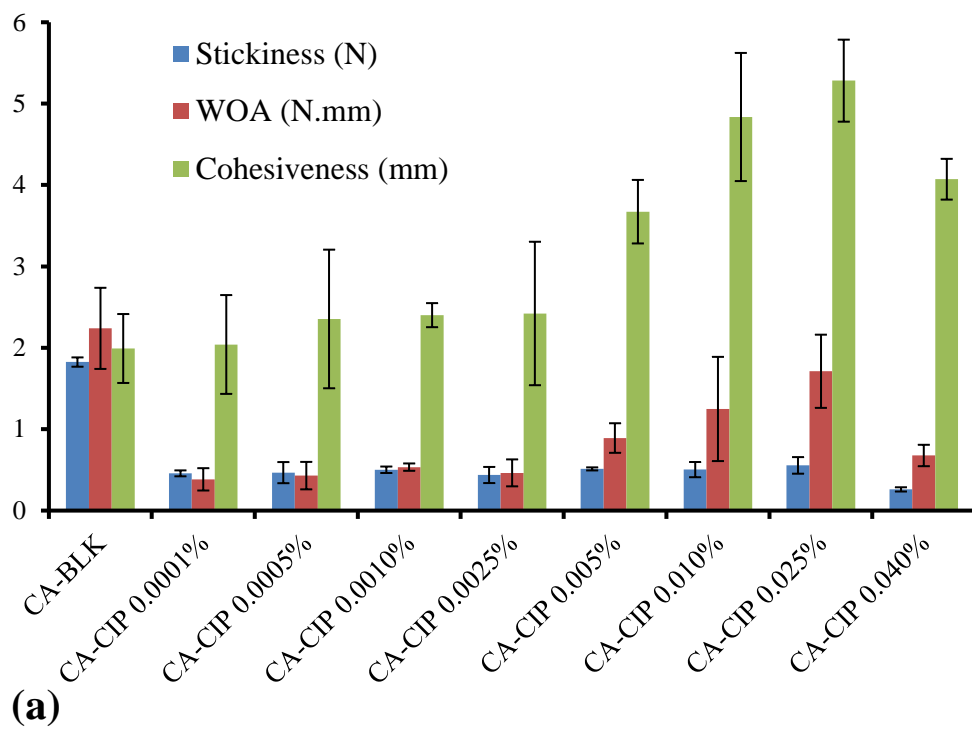


Figure 3 Hardness profiles of formulated wafers ($n = 3$) prepared from 1% w/w gels, compressed at three different places on both sides of the dressing showing effect of drug loading.



470

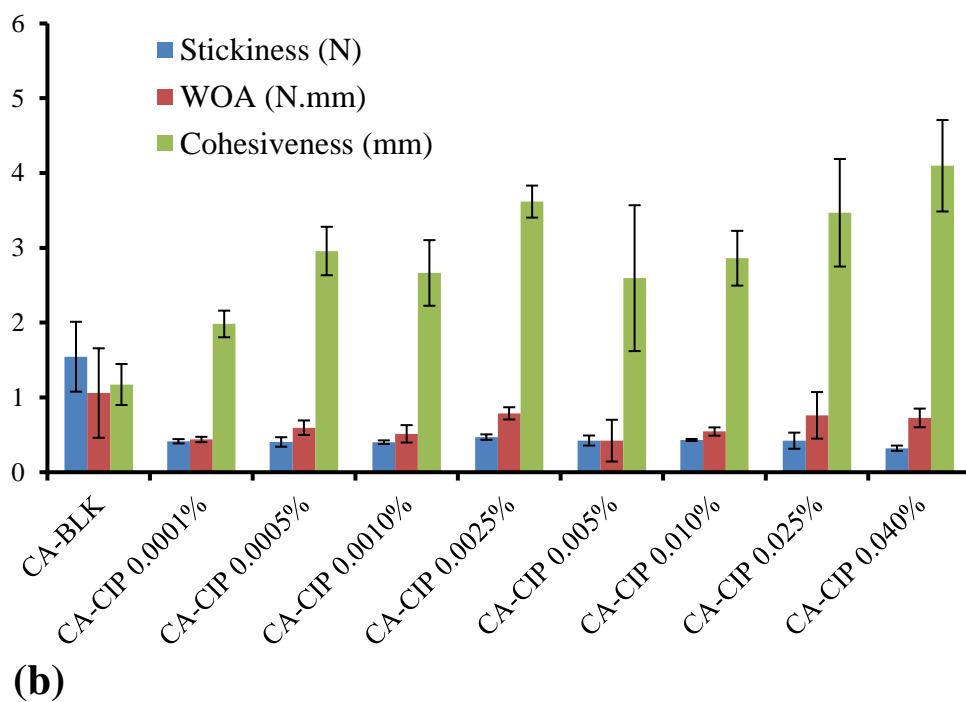
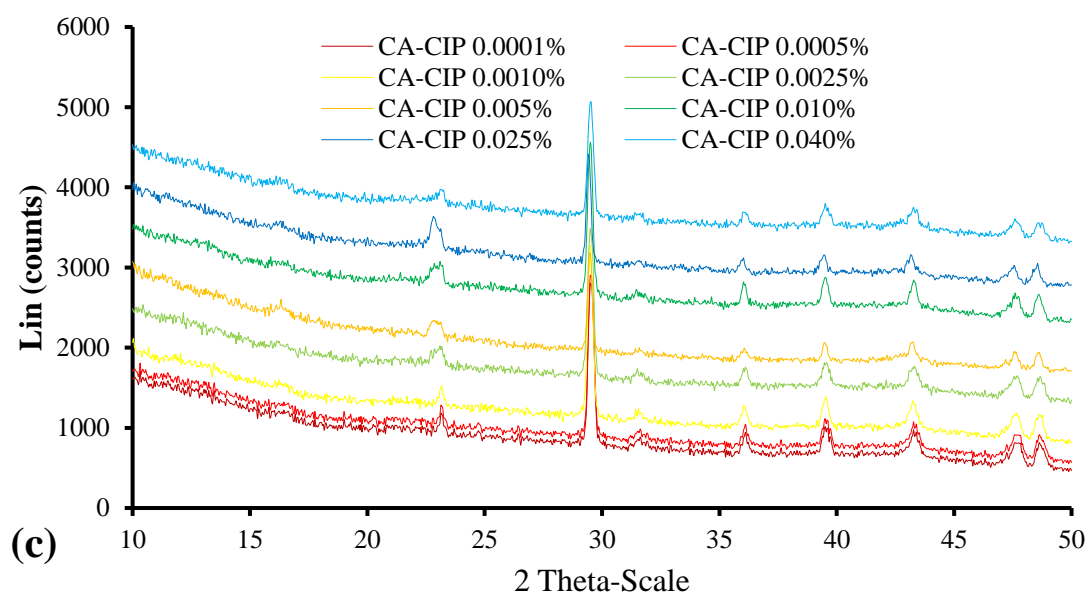
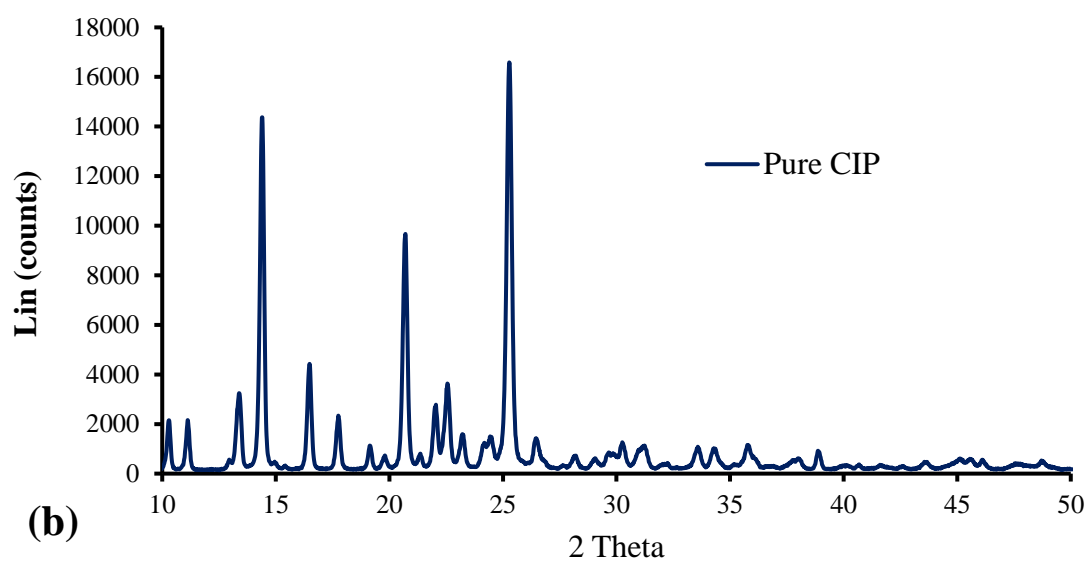
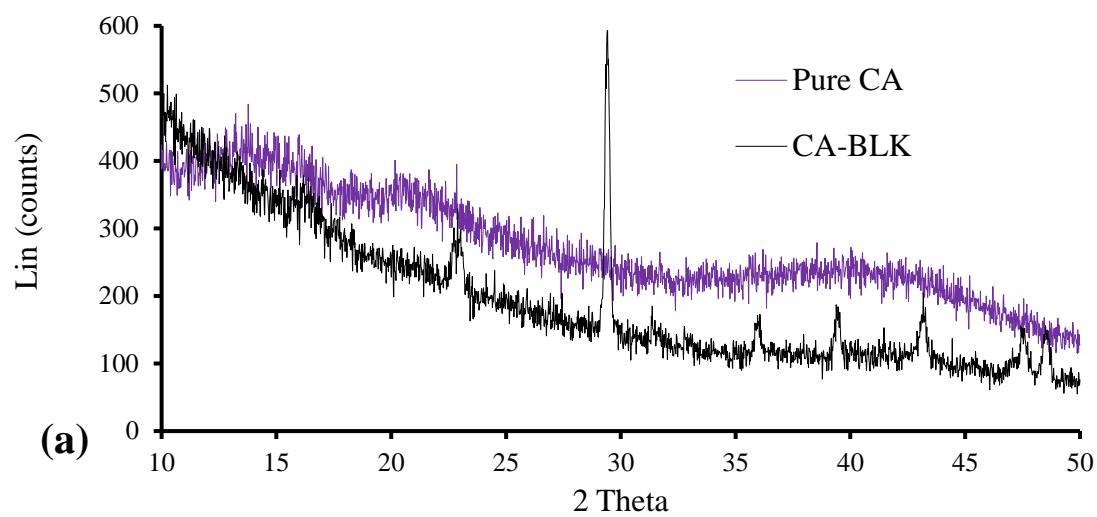


Figure 4 Adhesive profiles of CIP loaded wafers in the presence of (a) thin SWF containing 2% (w/w) BSA and (b) viscous SWF containing 5% (w/w) BSA.

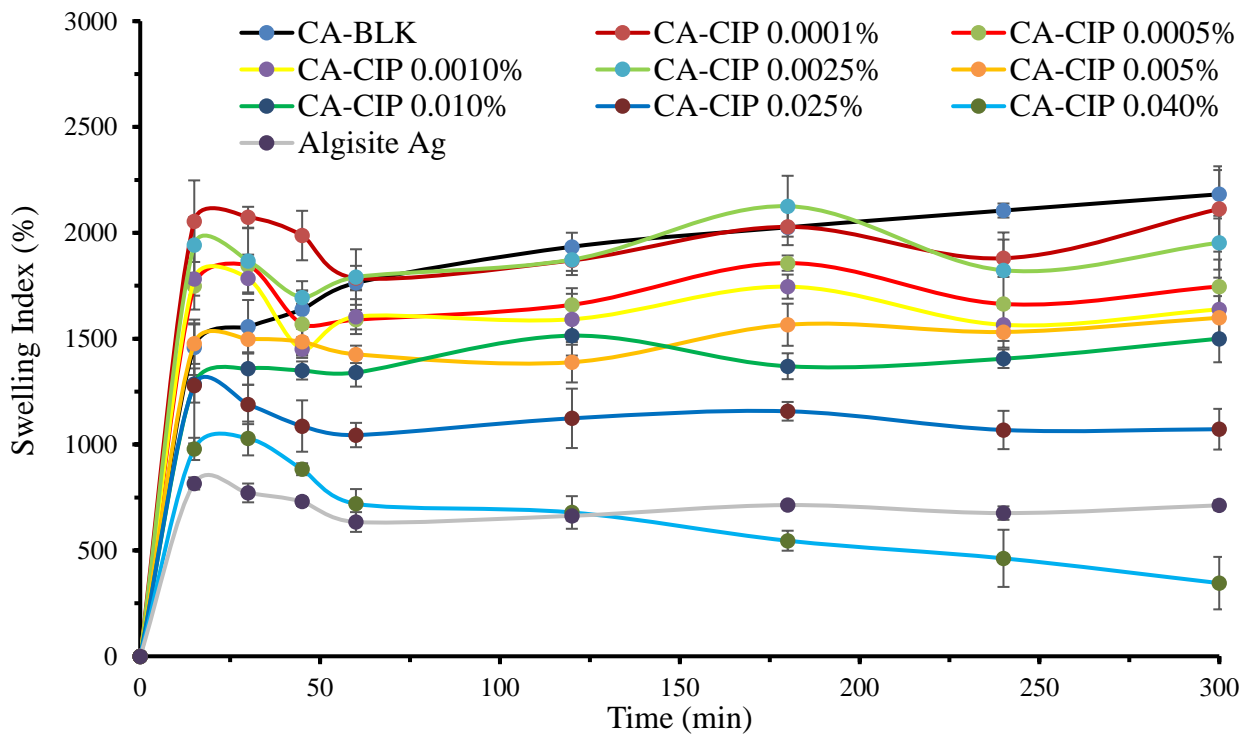


475

Figure 5 XRD patterns of (a) pure polymer and BLK wafer, (b) pure drug and (c) drug loaded wafers.

480

485



490

Figure 6 Swelling behavior of the different CA based dressings tested.

495

500

505

510

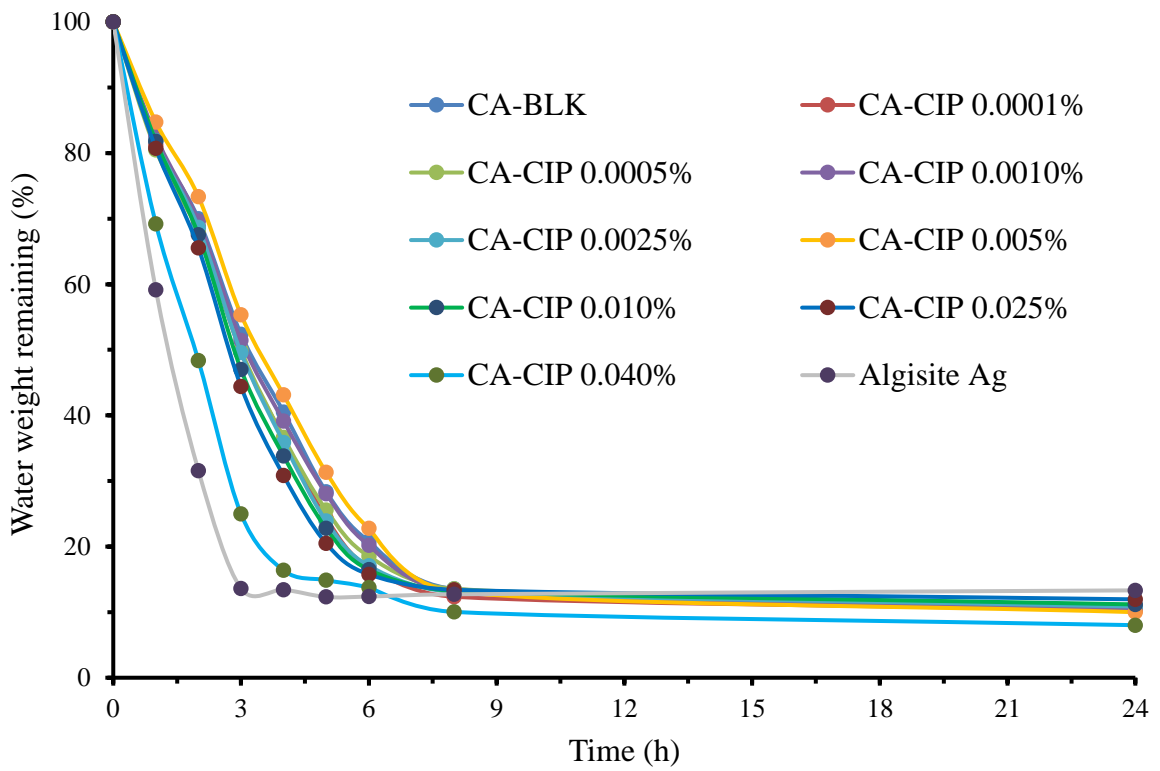
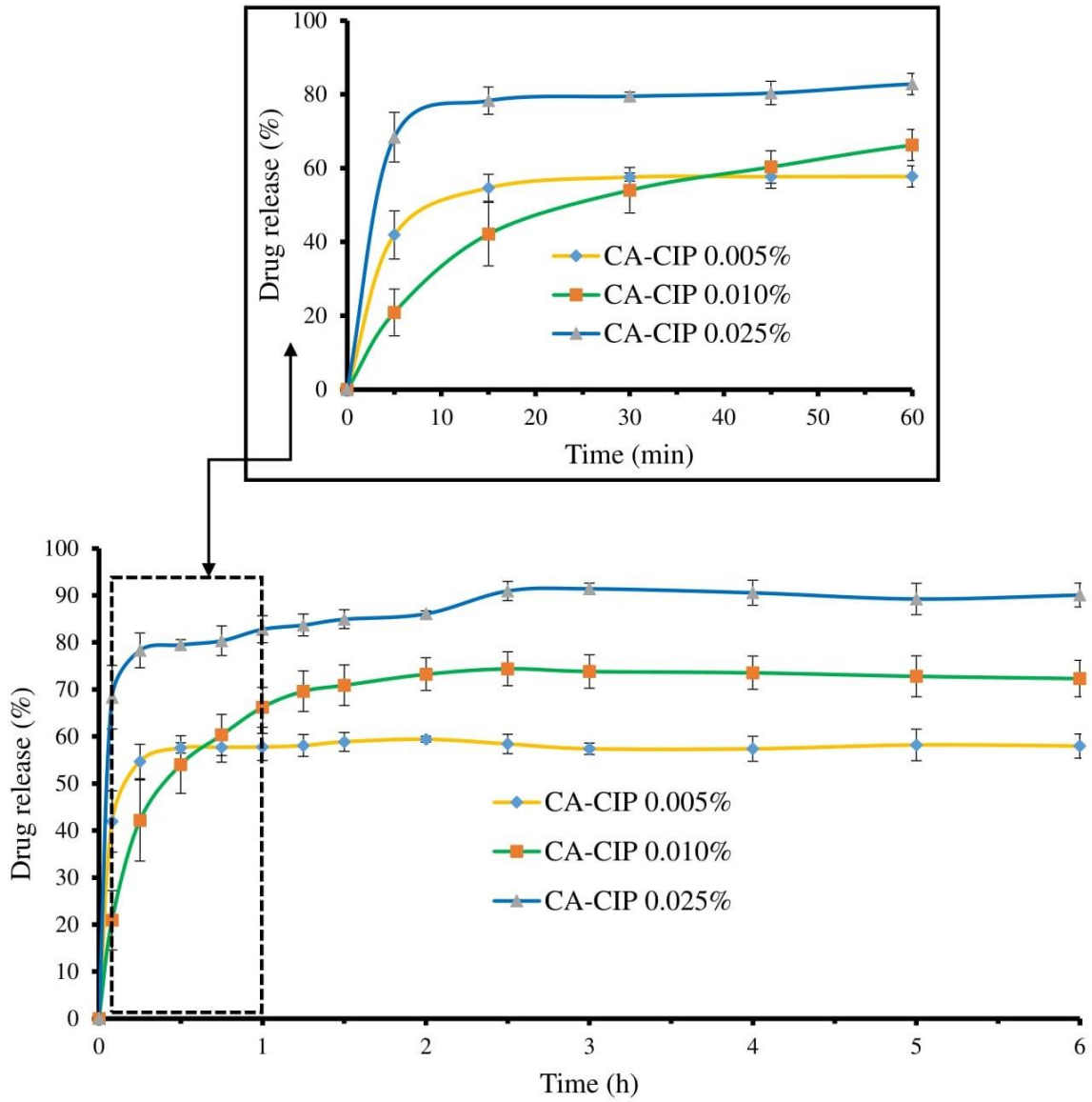


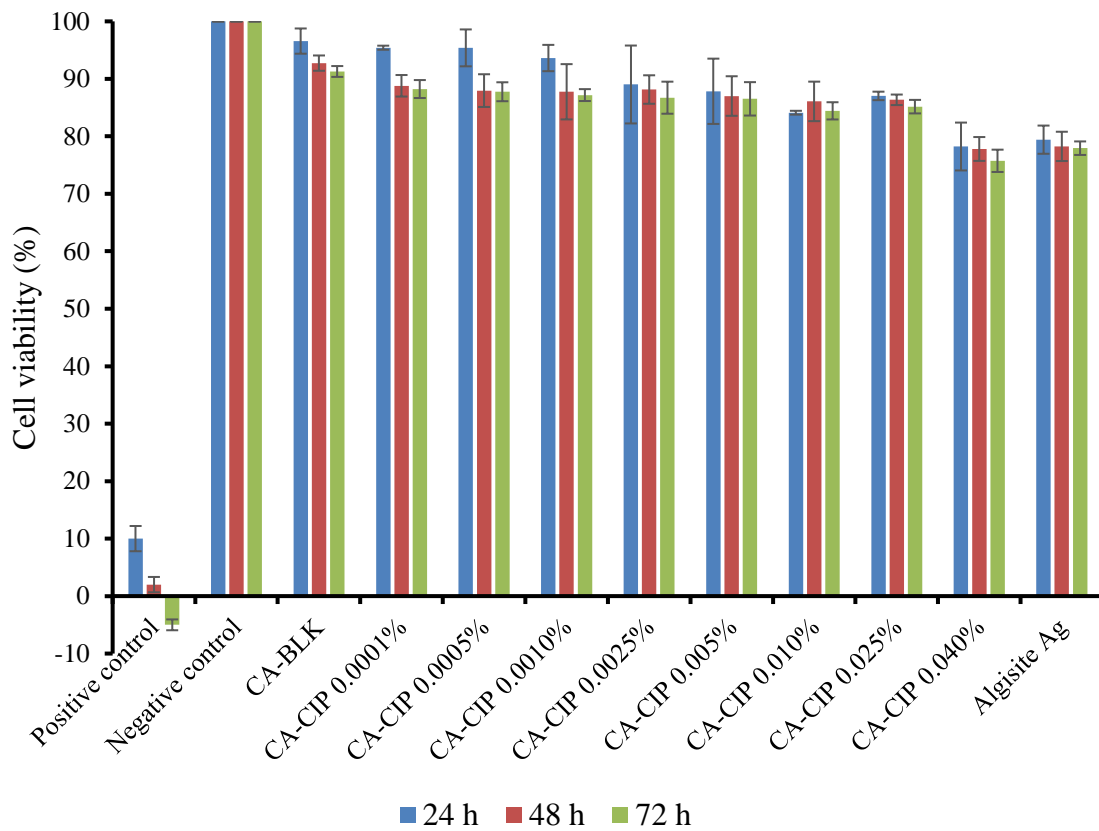
Figure 7 Evaporative water loss from Algisite Ag[®], BLK and DL wafers.



515 **Figure 8** Cumulative percentage drug release profiles of optimized CIP loaded wafers.

520

525



530

Figure 9 Cell viability of human primary epidermal keratinocytes after expositions to the extracts of CIP loaded wafers and fiber mat, Algisite Ag[®] for 24, 48 and 72 h (mean \pm SD, $n = 9$).